

Oxygen Regime Control in Water Body Amelioration

Valery Borovkov* and Ivan Karaichev

Moscow State University of Civil Engineering, Yaroslavskoe shosse, 26, Moscow, 129337, Russia

Abstract. An important aspect of water body amelioration is the control of the oxygen regime in water mass. Pollution of water bodies deteriorates their oxygen regime, and the natural inflow of oxygen through the free surface is not enough to compensate for oxygen consumption for pollutant oxidation. Water pollution by various substances causes damage resulting from a decrease in the ecological safety of urban water bodies. Data of World Health Organization (WHO) show that the contact of the population with polluted water bodies causes spreading of deceases, such as cholera, diarrhea, dysentery, hepatitis A, typhoid, and poliomyelitis, and creates considerable health risks.

In this context, the artificial aeration of water mass with the use of aeration systems, which improve water quality, is gaining in importance. Most widespread among such aeration systems are diffused-air aerators, in which air supplied by a compressor passes through perforated diffuser plates. The size of the perforation is often chosen with no appropriate hydraulic substantiation. The size of the resulting air bubbles, no doubt, depends on the size of perforation holes; however, the available design relationships give contradictory results depending on the immersion depth of the diffuser plate and the working pressure, which determines air discharge velocity from diffuser plate perforations. This shows that the studies along this line are of scientific and practical importance.

This article presents the analysis of the existing relationships for determining the size of air bubbles that form when air is pumped into water through nozzles of different diameters at different pumping rates; the analysis has shown the results of such calculations to differ considerably. Buckingham π -theorem was used to construct dimensionless groups, determining the relationship between the size of bubbles and the factors that govern the outflow of air into water. Dimensionless groups were used to obtain a formula for calculating the size of air bubbles at the aeration of water mass.

1 Introduction

The pollution of water bodies, especially in urban areas, disturbs their oxygen balance, shifts the ecological state of rivers and water bodies into the domain of anaerobic reactions, deteriorates the general ecological conditions of rivers and water bodies, and creates conditions for disturbing the environmental safety at the nearby areas [1]. One way to counteract these adverse trends can be the aeration of water masses. The rate of aeration

* Corresponding author: borovkov01@mail.ru

largely depends on the total contact surface of air bubbles and water mass, which depends on the size of air bubbles.[2,3]

The results of calculations of bubble sizes by formulas of different authors show that the dependence of bubble size on air velocity (Fig. 1) and nozzle diameter (Fig. 2) varies widely. [4]

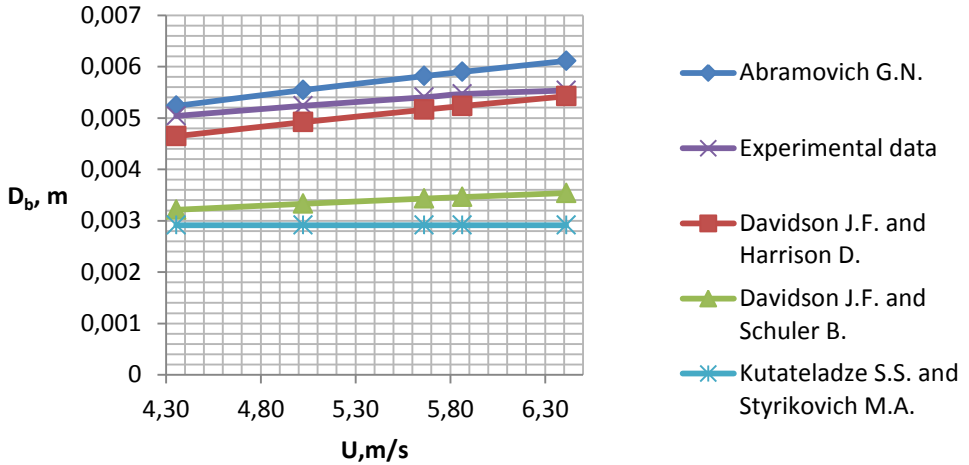


Fig. 1. The bubble size for nozzle diameter $d=0.00026$ m at different velocities as estimated by formulas of different authors (experimental data [5], Abramovich G.N. [6], Davidson J.F. and Harrison D. [7], Kutateladze S.S. and Styrikovich M.A. [8], and Davidson J.F. and Schuler B. [9]).

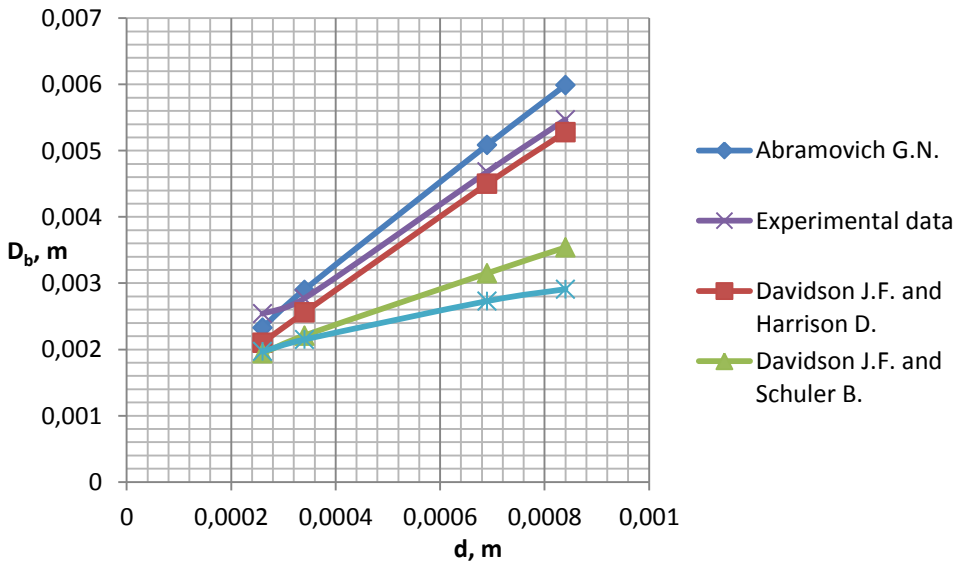


Fig. 2. The dependence of the size of a bubble D_b that forms at different nozzle diameters d and at gas discharge velocity of 6 m/s by formulas of different authors (Experimental data [5], Abramovich G.N. [6], Davidson J.F. and Harrison D. [7], Kutateladze S.S. and Styrikovich M.A. [8], and Davidson J.F. and Schuler B. [9]).

As can be seen from Fig. 1, the sizes of bubbles determined by theoretical models and experimental studies of different authors differ by factors more than 2.5. For example, the sizes of bubbles at different rates of air discharge through a nozzle with inner diameter $d=0.00026$ m differ by factors more than 3.

The analysis of calculation and analytical approaches and the comparison of the proposed formulas have shown that the proposed approaches are often contradictory and based on mutually exclusive assumptions; therefore, the formulas developed by different authors yield the results that differ several times. This shows that the issues of functioning of aeration systems for improving water quality and oxygen regime at the amelioration of water bodies are still not fully understood.[10]

The objective of this study is to specify the regularities of formation of air bubbles at air pumping into water mass.

2 Method of study

The problems were solved by an experimental–analytical method, implying the use of theoretical models and calculation–analytical approaches combined with experimental determination of variables that cannot be estimated otherwise.

The formation of air bubbles in water from air pumped through submerged holes is a complex process, depending on many factors, which make it difficult to describe theoretically. [11, 12]

The size of the bubbles forming in this process D_b depends on the following characteristics: nozzle diameter d , water density ρ_l , air discharge velocity u , air density ρ_g , the interfacial tension of water σ , gravitational acceleration g , and the kinematic viscosity of water ν ; these characteristics can be related by the following function:

$$D_b = \varphi(d, \rho_l, u, \rho_g, \sigma, g, \nu) \quad (1)$$

or as

$$\varphi(d, \rho_l, u, \rho_g, \sigma, g, \nu, D_b) = 0 \quad (2)$$

Using the Buckingham π -theorem [13] and taking nozzle diameter d , liquid density ρ_l , and air discharge velocity u as the factors to be raised to some powers, which are to be determined, we combine the interrelated physical characteristics to obtain the following five dimensionless groups:

$$\pi_1 = d^{x_1} \cdot \rho_l^{y_1} \cdot u^{z_1} \cdot \rho_g = \frac{\rho_g}{\rho_l} \quad (3)$$

$$\pi_2 = d^{x_2} \cdot \rho_g^{y_2} \cdot u^{z_2} \cdot \sigma = \frac{\sigma}{d \cdot \rho_g \cdot u^2} = We^{-1} \quad (4)$$

$$\pi_3 = d^{x_3} \cdot \rho_g^{y_3} \cdot u^{z_3} \cdot g = \frac{d \cdot g}{u^2} = Fr^{-1} \quad (5)$$

$$\pi_4 = d^{x_4} \cdot \rho_g^{y_4} \cdot u^{z_4} \cdot \nu = \frac{\nu}{d \cdot u} = Re^{-1} \quad (6)$$

$$\pi_5 = d^{x_5} \cdot \rho_g^{y_5} \cdot u^{z_5} \cdot D_b = \frac{D_b}{d} \quad (7)$$

The functional equation incorporating the obtained dimensionless parameters can be written as

$$\frac{D_b}{d} = \varphi \left(\frac{\rho_g}{\rho_l}, We^{-1}, Fr^{-1}, Re^{-1} \right) \quad (8)$$

This analysis allows the parameters to be combined by multiplying them by any constant, raising them into any power, or combining by their multiplication [14]. Thus, the parameter π_4 raised to power -1 and multiplied by π_5 becomes the Reynolds number:

$$(\pi_4)^{-1} \cdot \pi_5 = \left(\frac{\nu}{d \cdot u} \right)^{-1} \cdot \frac{D_b}{d} = \frac{D_b \cdot u}{\nu} = Re_b \quad (9)$$

where bubble diameter D_b is used instead of pore diameter d_p as a geometric characteristic.

Now, with the use of the obtained dimensionless groups, the functional equation can be written as:

$$\frac{D_b}{d} = \varphi \left(\frac{\rho_g}{\rho_l}, We^{-1}, Fr^{-1}, Re_b \right) \quad (10)$$

This form of equation gives no information about the function itself, but it allows the researcher to rationally organize the experimental study and the generalization of experimental data.

The form of the function was determined based on the experimental studies on the installation schematized in Fig. 1.

Air from compressor (1) is directed to the rubber receiver (2) to smooth the possible pressure pulsations created by the piston-type compressor. From the receiver, air runs through a high-pressure line, the pressure regulator (3), and the control valve (4) to reach the vertical nozzle (6) placed in the rectangular vessel (7); the characteristics of the forming bubbles are recorded by the still camera (8) and the high-speed videorecorder (9); water temperature and dissolved oxygen content are transmitted by the sensor (10) to the dissolved-oxygen device (11) and recorded in the notebook (12).

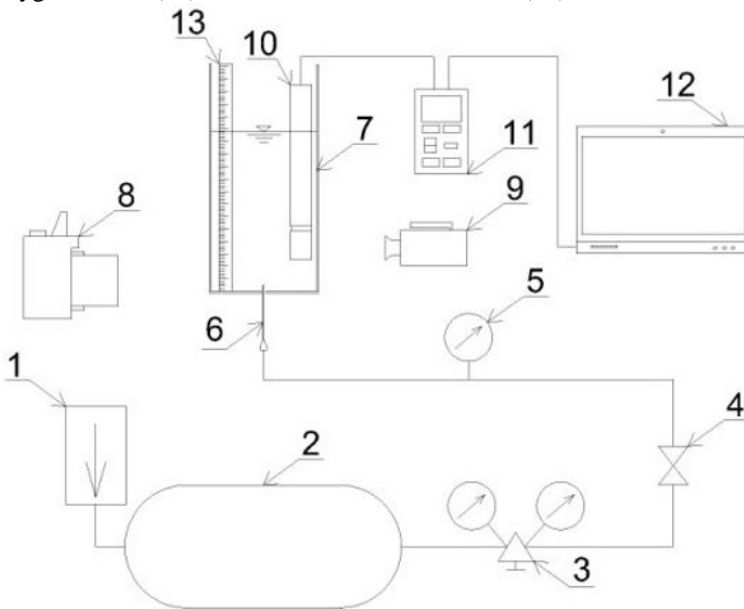


Fig. 3. Experimental installation scheme

The nozzles of different inner diameters were medical needles of different size, the outlet section of which had been cut perpendicular to the axis of the needle. The ratio of the nozzle length to its diameter $\frac{L_n}{a} > 100$. This length-to-diameter ratio is commonly assumed to be sufficient for the perturbations at the entry of air flow into the nozzle to be attenuated and thus to have no effect on the bubble-formation process. [15]

Table 1. Characteristics of the needles used in the study.

Needle gage	Outer diameter, mm	Inner diameter, mm	Wall thickness, mm
18	1.27	0.838	0.216
19	1.067	0.686	0.191
20	0.9081	0.603	0.1524
21	0.8192	0.514	0.1524
22	0.7176	0.413	0.1524
23	0.6414	0.337	0.1524
25	0.5144	0.26	0.1524

The linear scale in the photo images and video records is given by a ruler placed in the vessel in plane with the air-supply nozzle. Such arrangement eliminates linear errors.

The obtained photo images were processed in AutoCAD package to construct a three-dimensional model of the bubble (Fig. 3) as a rotation body with the subsequent calculation of its volume and an equivalent sphere diameter, which was used in the further analysis and generalization of experimental data.



Fig. 4. A photograph of a bubble and its 3D model.

The discharge of air through the nozzle was determined in the course of experimental data processing as the product of the volume of produced bubbles multiplied by their formation frequency. Accordingly, the ratio of air discharge rate to the outlet area was used to evaluate the velocity of air supply.

The rate of air supply was kept stable by using a rubber receiver to attenuate the internal oscillation of air caused by the pulsating operation of the compressor. The installation creates an internal pressure of 4 atm, which is reduced in a gas pressure reducer to a stable working pressure between 1000 and 5000 Pa. This pressure is enough to overcome the hydraulic resistance in the feed main and the nozzle, the local resistances, and the forces

that hamper air input into the water mass, such as hydrostatic pressure, surface tension, and the hydrodynamic resistance to the displacement of bubble boundary during its growth.

The operating pressure, which determines the air discharge, was controlled by an inclined micromanometer MMN-2400 connected with the low-pressure line. This instrument features the first class of accuracy and ensures high-sensitivity measurement control.

The operation pressure was controlled by a control valve, mounted in the line after the reducer (Fig. 1) and enabling the pressure in the system to be adjusted by air bleeding.

The lower boundary of the measurements of bubble parameters corresponded to the initial pressure at which bubble formation began. The upper pressure limit corresponded to the regime of formation of single bubbles [16]. In the course of studies, the regime of formation of single bubbles was considered, which is the most widespread at the use of pneumatic aeration. [17,18]

3 The obtained results

The measurements of the sizes of the bubbles that form in the experiment were used to vary the governing criteria of Reynolds and Weber within a wide range (Table 2). These criteria were applied to generalize experimental data in the form of a single relationship $lgRe_b = f(lgWe)$.

Table 2. Variation boundaries of the governing criteria

Group	Re_b	We
min	300	0.12
max	2700	4.4

Note that the parameter $\pi_1 = \rho_l / \rho_g$ did not change in the experiment; therefore, it is not present in the obtained relationships. The Froude number, including air discharge velocity squared, the nozzle diameter, and the constant acceleration due to gravity does not enter separately in the obtained relationships, because the parameters that enter the Froude number are reflected in the criteria Re_b and We . This is why the separate effect of the Froude number on the formation of air bubbles was not identified in the experiment.

The experimental results are given in Fig. 3 as a plot of function $lgRe_b = f(lgWe)$, combining the data obtained in experiments with air injection into a liquid at rest through nozzles with different internal diameters.

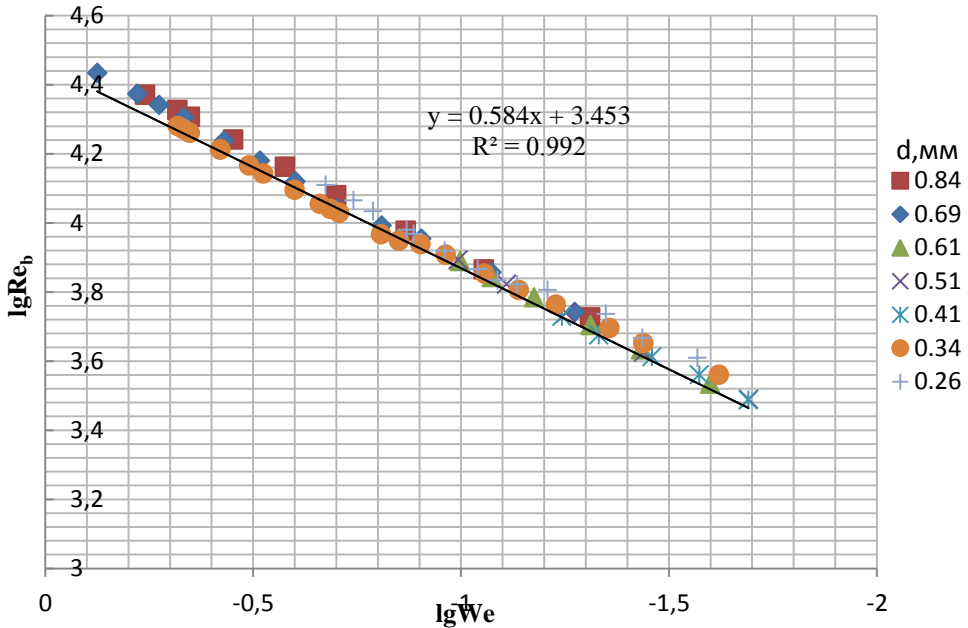


Fig. 5. Generalized experimental data in dimensionless form

The coordinates of similarity, obtained above by the dimensional method were used to generalize the entire body of experimental data and to obtain a universal relationship for the conditions of the experiments.

$$\lg Re_b = 0.584 \lg We + 3.5 \quad (11)$$

This relationship can be also presented in a power form:

$$Re_b = 3162 We^{0.584} \quad (12)$$

4 Conclusions

The dimensional analysis was applied to a group of factors governing the process of bubble formation when air is injected into a liquid at rest to establish that the size of the air bubbles released from the nozzle can be found from a relationship between the Weber number and Reynolds number. The analysis of experimental data based on a criterial relationship obtained with the use of Buckingham π -theorem was used to generalize the measurement data and to obtain a dimensionless relationship for calculating the ratio of the diameter of air bubbles to nozzle diameter for different conditions of air injection into the water mass in the calculation of aeration devices and the regulation of their operation regime to achieve the best amelioration effect [19, 20].

References

1. Karelin V.Y., Borovkov V.S., Volshanik V.V., Galant M.A., Dorkina I.V. Engineering system to maintain the quality of water ponds. Bulletin of the Department of Building Sciences, 2001. Vol. 4, pp. 28-35.

2. Ksenofontov B.S. Flotation treatment of water, waste and soil. Moscow: New Technologies, 2010. pp 272.
3. McCann D.J., Prince RGH. Regimes of bubbling at a submerged orifice. Chem Eng Sci, 1971. Vol 26, pp. 1505-1512
4. Borovkov V. S., Karaichev I. E., Hydrophysical factors affecting the formation of bubbles during water aeration. Ecology of urban areas. 2017, № 4, c. 32-35;
5. Karaichev, I.E., Factors that influence the process of bubble formation at air injection into a liquid at rest, Development of technical sciences in the modern world, 2016, pp. 91–94.
6. Abramovich, G.N., Hydrodynamics of underwater air curtains, Itogi Nauki Tekh., Ser.: Mekh. Zhidk. Gaza, 1986, vol. 20, pp. 85–92.
7. Davidson, J.F., Harrison, D., Pseudo-liquefaction of Solid Particles, Khimiya, 1965.
8. Kutateladze, S.S., Styrikovich, M.A., Hydraulics of Gas–Liquid Systems, Moscow–Leningrad: Energiya, 1976.
9. Davidson, J.F., Schuler B.O.G., 1960. Bubble formation at an orifice in a viscous liquid, Trans. Inst. Chem. Eng., 38, 144–154, 335-342
10. Rzasz R., Joanna Boguniewicz-Zablocka. Analysis of gas bubble formation at the nozzle outlet. ECOL CHEM ENG A., 2014. Vol. 21 No. 4, pp. 493-502.
11. McCann D.J., Prince RGH. Regimes of bubbling at a submerged orifice. Chem Eng Sci, 1971. Vol 26, pp. 1505-1512.
12. Brounshtein, B.I., Hydrodynamics, Mass and Heat Exchange in Towers, Leningrad: Khimiya, 1988.
13. Makarov, V.A., and Menzin, A.B., Simulation of Oceanographic Processes, M.–L., 1979.
14. Sharp D. Hydraulic modeling M: Moscow “Mir” 1984 C.49-54
15. Karaichev I. E. Methods and techniques for the experimental study of the formation of bubbles when air is blown into the liquid. Scientific Review. 2017, № 7, c. 64-68;
16. Miyahara T., Takahashi T. Bubble formation in single bubbling regime with weeping at a submerged orifice. Chem Eng Jpn., 1984. Vol. 17 No. 6, pp. 597–602.
17. Sukharev I.S. Experimental determination of the size of gas bubbles during the outflow in the air-water system. Bulletin of the Volga State Academy of Water Transport, 2016. pp. 198 - 204.
18. Ksenofontov B.S. Flotation treatment of water, waste and soil. Moscow: New Technologies, 2010. pp 272.
19. Meshengisser Yu. M. Theoretical justification and development of new polymer aerators for biological sewage treatment. Dis. Doctor of Technical Sciences FGUP "NII VODGEO". Moscow, 2005.
20. Boshenyatov B. V., Microbubble gas-liquid environments and prospects for their use, Lambert, 2016, pp 170